

Generation and cessation of oscillations: Interplay of excitability and dispersal in a class of ecosystem

Ramesh Arumugam,¹ Tanmoy Banerjee,^{2, a)} and Partha Sharathi Dutta^{1, b)}

¹⁾ *Department of Mathematics, Indian Institute of Technology Ropar, Rupnagar 140 001, Punjab, India.*

²⁾ *Chaos and Complex Systems Research Laboratory, Department of Physics, University of Burdwan, Burdwan 713 104, West Bengal, India.*

(Dated: 30 September 2018; Received :to be included by reviewer)

We investigate the complex spatiotemporal dynamics of an ecological network with species dispersal mediated via a mean-field coupling. The local dynamics of the network are governed by the Truscott–Brindley model, which is an important ecological model showing excitability. Our results focus on the interplay of excitability and dispersal by always considering that the individual nodes are in their (excitable) steady states. In contrast to the previous studies, we not only observe the dispersal induced generation of oscillation but we also report two distinct mechanisms of cessation of oscillations, namely amplitude and oscillation death. We show that, the dispersal between the nodes influences the intrinsic dynamics of the system resulting multiple oscillatory dynamics such as period-1 and period-2 limit cycles. We also show the existence of multi-cluster states which has much relevance and importance in ecology.

Species dispersal among connected habitats often identifies the complex spatial dynamics of ecological system and significantly increases the persistence of ecological communities for longer time. Various dynamical models have been used to describe the effect of dispersal in connected habitats. As far as ecological models are concerned, sometimes there exists slow-fast time scales with very interesting dynamics. For example, in aquatic ecosystem, plankton bloom is a result of sudden changes in environmental fluctuations that makes plankton ecosystem as excitable media. Take this into account, the effect of dispersal in slow-fast dynamical ecological system is analyzed qualitatively using mean-field assumption as an external force. In a homogeneous environmental set up, the coupled slow-fast system shows multiple characteristics of sensitivity in synchronized oscillations for different initial density.

an external perturbation^{2,3}. In most of the physical and biological systems, excitation arises with various dynamical aspects. In particular, in neuronal systems, two main types of excitability are defined, namely type-I and type-II excitability. The type-I excitability is characterized by the appearance of a stable limit cycle with arbitrarily low frequency via a global bifurcation^{4,5}. On the other hand, the type-II excitability yields zero-amplitude and finite period spikes through the supercritical Hopf bifurcation⁶.

Although, the notion of excitability has been well studied in the context of neuronal systems⁷, it remains less explored in the field of ecology, where excitability plays an important role in maintaining species diversity, e.g., in aquatic ecosystems⁸. As far as the excitable ecological systems are concerned, external perturbation arises naturally in the form of demographic rates⁹, environmental fluctuations^{10,11}, seasonal variation¹², and even migration of populations^{13,14}. Therefore, it is of natural interest to explore the role of excitability in ecological systems.

Furthermore, like neurons, ecological systems are also rarely isolated¹⁵. The dispersal of species through an external force often connects the fragmented habitats¹⁶ which subsequently promotes the synchronized oscillations¹⁷. In other words, the connectivity of habitats through migration (coupling) enhances the relationship between synchrony and stability. Hence, it is of broad interest to examine the collective behaviors of interacting excitable ecological units. In literature, a large number of studies have been devoted to explore the collective behaviors of excitable units in biology, such as, neurons, genetic oscillators, beta cells in islets of Langerhans, etc⁷. In all these studies, interaction takes place in a *microscopic scale*, e.g., through the sharing of membrane voltage or diffusion of ions. Depending upon the underlying mechanisms of the individual nodes and their organization, these interactions are governed by coupling topology. Therefore, the natural question to ask is how

I. INTRODUCTION

Excitability is one of the interesting features of slow-fast dynamical systems that is characterized by the fact that a small perturbation in the input leads to a large excursion in phase space before coming to the rest state¹. Notably, an excitable medium possesses stable equilibria which exhibits qualitatively different behavior (large excursion in the phase space) according to the character of

^{a)}Electronic mail: tbanerjee@phys.buruniv.ac.in

^{b)}Corresponding author

; Electronic mail: parthasharathi@iitpr.ac.in

the similar types of coupling functions affect the collective behaviors of an excitable system in a *macroscopic scale* such as an *ecological network* with excitable units? This study is relevant since in both the biological and ecological networks the types of interactions are quite identical: For example diffusion or quorum sensing mechanism through ions in biology is equivalent to the dispersal or weighted mean-field dispersal of species density in an ecological system. Therefore, in the present study we try to reveal the following important questions: Does the generation of oscillation rely on the characteristics of excitable system or type of coupling we used in? What is the effect of dispersal on the dynamics of excitable ecological systems? What are the new dynamical features involved in this coupled excitable systems?

To address these questions, we emphasize on the excitable system's features by considering an ecological system, namely the "Truscott–Brindley model" with species spatial movement. In the context of ecological systems, the Truscott–Brindley model determines the excitability due to fluctuating weather conditions with demographic and environmental noise as perturbations¹⁸. Concerning the external forces of an ecological system, here we use mean-field coupled Truscott–Brindley model as a consumer–resource model in which migration of populations takes place among the selected habitats and preserves the fundamental characteristics of an excitable system. Generally, this mean-field assumption is used as a diffusive coupling in physical^{19–21}, biological²² as well as in ecological systems¹⁷ to quantify the average distribution. In contrast to excitable oscillations, in this paper we show that the oscillatory behaviour of individual patches are suppressed through two distinct mechanisms, namely amplitude death (AD) and oscillation death (OD). In general, the oscillation quenching mechanisms such as AD and OD play important roles to suppress the oscillations in most of the physical, chemical and biological oscillators²³. Basically, AD is the mechanism by which two or more interacting oscillators arrive at a common homogeneous steady state, whereas in OD oscillators populate different branches of stable inhomogeneous steady states which are created by symmetry breaking in the network^{23,24}. The OD state is particularly important from biological point of view as it induces inhomogeneity in an otherwise homogeneous network that has relevance in biology, e.g., in synthetic genetic oscillator^{25,26} and cellular differentiation²⁷. It should be noted that although the occurrence of AD has been reported earlier in excitable ecological oscillators under conjugate coupling²⁸ but this is the first time we reveal the occurrence of oscillation death and other interesting behavior, such as, multi-cluster oscillation death. With the presence of active and passive dispersal in homogeneous and heterogeneous habitats we further reveal the multiple characteristics of excitable system such as generation of oscillation and transition from period-1 to period-2 limit cycle with certain threshold value in the parameter.

The outline of this paper is as follows. First, in Sec. II,

we explain the uncoupled and the coupled TB model with dispersal in only consumer population. In Sec. III, with variations in physiological and environmental parameters, various qualitative behaviours of dispersal effect with appearance and disappearance of oscillations are described for identical and non-identical patches. Following that, bidirectional coupling is taken into account, various dynamical consequences of dispersal and excitability are illustrated in Subsec. III D. Finally, to check the robustness of coupled excitable system, a network of few patches is analyzed and thereafter we have the discussion and concluding remarks in Sec. IV.

II. MATHEMATICAL MODEL

To study the consumer-resource interactions with the excitable (i.e., slow-fast) local dynamics in a patchy habitat (i.e., spatially extended population), we consider the Truscott–Brindley model in each of the patches. The Truscott–Brindley model exhibits type-II excitability, and is known to mimic plankton blooms in ecosystems⁸.

A. Non-dimensionalized Truscott–Brindley Model

We start with the dimensionless form of the Truscott–Brindley model^{8,29}. The dynamics of the resource (X) and the consumer (Y) with their associated interactions are given by the below equations:

$$\frac{dX}{dt} = f(X, Y) = \beta X(1 - X) - Y \frac{X^2}{X^2 + \nu^2}, \quad (1a)$$

$$\frac{dY}{dt} = g(X, Y) = \gamma \left(\frac{X^2}{X^2 + \nu^2} - \omega \right) Y, \quad (1b)$$

where β is the maximum growth rate of the resource (X), ν is half saturation constant of the consumer (Y) which governs how quickly maximum predation rate is attained as density of the resource increases, γ is the maximum growth rate of the consumer (Y) or the conversion efficiency rate of the ingested resource due to predation and further ω represents the consumer's mortality rate. The growth of the resource (X) is characterized by the logistic growth function and grazing by the consumer (Y) is represented by the Holling type-III functional response³⁰. The model (1) has equilibrium point and oscillatory states for different parametric set up. To exhibit slow-fast dynamics the value of ν must stay in the parameter range: $0 < \nu < \frac{1}{3\sqrt{3}} = 0.1924$. This parametric range ensures that the nullcline $f(X, Y) = 0$ has two turning points (one local maxima and one local minima) those are instrumental for the system to exhibit slow-fast dynamics (see Fig. 1). Another parameter which governs the qualitative behaviour of the model (1) is ω . Since the position of the nullcline $g(X, Y) = 0$ is determined by the value of ω . The other two parameters γ and β do not have much influence on the qualitative behavior of

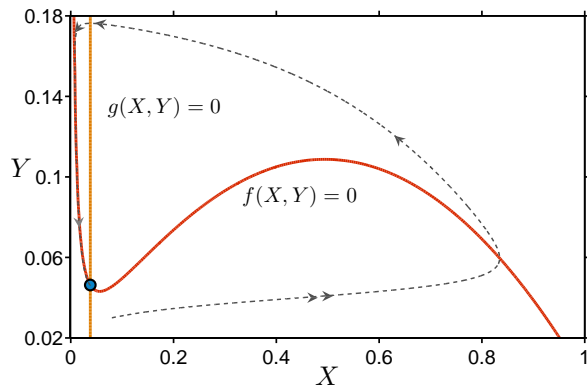


FIG. 1. (Color online) Nullclines of the resource (X) and the consumer (Y) populations in the uncoupled Truscott–Brindley model (1) are shown here for fixed parameters $\gamma = 0.05$, $\omega = 0.34$, $\nu = 0.053$ and $\beta = 0.43$. The red curve represents the resource equation (1a), whereas the orange line represents the consumer equation (1b). The solid circle represents the equilibrium point. The dashed arrow marked curve shows how an initial condition approaches the equilibrium point.

the Truscott–Brindley model⁸. An exemplary parameter values for an equilibrium point are: $\beta = 0.43$, $\nu = 0.053$, $\gamma = 0.05$ and $\omega = 0.34$. To identify the collective dynamics of coupled excitable system, we use this parameter values so that each uncoupled system (1) has only fixed point state. However, to have oscillations in the uncoupled model (1), the value of ω needs to be changed accordingly.

B. Coupled Truscott–Brindley Model

In nature, it is commonly understood that the species diversity in spatially fragmented habitats can be preserved by the movement of populations from nearby patches. Such movement or dispersal of populations between spatially separated patches is potentially important for the survival and persistence of the community³¹. Without dispersal, the consumer–resource dynamics in a single patch is represented by the uncoupled Truscott–Brindley model Eq. (1). Here species spatial movement among N number of patches is taken into account, firstly we couple only the consumer populations (Y) in each patch using the mean-field dispersion¹⁷. Therefore, the coupled model due to species movement is given by:

$$\frac{dX_i}{dt} = \beta X_i(1 - X_i) - Y_i \frac{X_i^2}{X_i^2 + \nu^2}, \quad (2a)$$

$$\frac{dY_i}{dt} = \gamma \left(\frac{X_i^2}{X_i^2 + \nu^2} - \omega \right) Y_i + \epsilon (Q\bar{Y} - Y_i), \quad (2b)$$

where $i = 1, 2, \dots, N$ and $\bar{Y} = \frac{1}{N} \sum_{i=1}^N Y_i$. The parameter ϵ represents the coupling strength (or the dispersal

rate) of the consumer (Y) and Q represents the mean-field density of the consumer which quantifies the average distribution of density in the patches. In fact, this mean field density (Q) determines the qualitative and the quantitative behavior of migrated consumer populations among the selected patches^{17,32}. Each i -th patch has two distinct dynamical features. One is populations local dynamics within a patch where population density is quantified due to interaction between the resource and the consumer. Another one is dispersal dynamics due to mean-field coupling or exchange of individuals in consumer populations (Y) between the patches. Depending on species density in each patch, the consumer movement can be either emigration or immigration in their respective patch.

III. RESULTS

We analyze this excitable system starting with nullclines of the uncoupled dimensionless model (1). In Fig. 1, we show the nullclines of the consumer and the resource. Intersection of this two nullclines is an equilibrium point of the considered model (1). Also the qualitative behavior of phase space can be easily identified using these nullclines. The dashed curve in Fig. 1 exhibits how a trajectory in (X, Y) phase plane approaches the equilibrium point following two different time scales (fast along the X axis and slow along the Y axis). Further, linear stability analysis of the coupled system (2) is performed wherever possible, otherwise numerical bifurcation analysis is carried out using XPPAUT³³ package by adopting a suitable method for stiff systems.

A. Dynamics of the uncoupled system

The small value of ν ($= 0.053$) ensures that the system has a slow-fast dynamics. For low mortality rate of the consumer (i.e., $\omega = 0.34$) in the uncoupled model (1), no oscillation occurs and populations exist only in the excitable steady state. In Fig. 2(a), we have shown a one-parameter bifurcation diagram for varying the mortality rate (ω) of the consumer using the uncoupled Truscott–Brindley model. From Fig. 2(a), it is clear that oscillation starts beyond a certain mortality rate, say the Hopf bifurcation point ω_H (here $\omega_H = 0.528$) in the uncoupled model (1). In the shaded region, there exists no oscillation other than excitable steady states. We show temporal dynamics of the model (1) in Fig. 2(b) that indeed shows the occurrence of steady state after a brief transient episode.

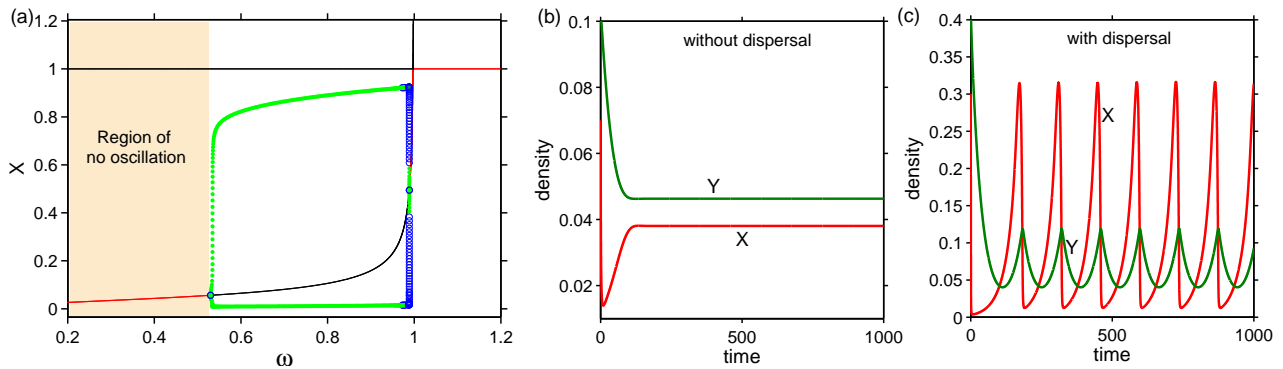


FIG. 2. (Color online) (a) One parameter bifurcation diagram for varying ω of the uncoupled model (1). Here shaded region represents the occurrence of steady state. Green and blue circles represent stable and unstable limit cycles respectively, whereas red and black curves represent the stable and unstable steady states. (b) Time series of both resource (X) and consumer (Y) of the uncoupled model (1) for $\omega = 0.34$. (c) For $\omega = 0.34$, time-series of both the resource (X) and consumer (Y) in the presence of dispersal when the dispersal rate $\epsilon = 0.2$ and the mean-field density $Q = 0.95$. Other parameter values in (a)-(c) are $\gamma = 0.05$, $\nu = 0.053$ and $\beta = 0.43$.

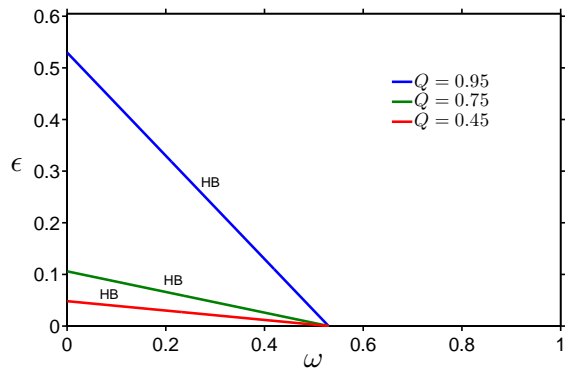


FIG. 3. (Color online) Two-parameter bifurcation diagram for different mean-field density Q : $Q = 0.45$, $Q = 0.75$, and $Q = 0.95$; $\omega - \epsilon$ space is shown where the Hopf bifurcation (HB) curve separating two different regions of equilibrium point and oscillation. HB curve represents the point where the oscillation starts due to the coupling, below HB curve is the region where only steady states occur and above HB curve is the region of both appearance and disappearance of oscillations. Other parameter values are $\gamma = 0.05$, $\nu = 0.053$ and $\beta = 0.43$.

B. Dynamics of the coupled system: Identical patches

1. Patches are in excitable steady state: Effects of dispersion

We consider that the patches are in excitable steady states and examine the effect of dispersion on the coupled dynamics. Let us start with an exemplary scenario of generation of rhythm from the steady state that is induced by the dispersal between the patches: We take $\omega = 0.34$ which is less than ω_H and uncoupled dynamics are in the excitable steady state (c.f. Fig. 2(b)). In the presence of dispersal ($\epsilon = 0.2$) and mean-field density

($Q = 0.95$) (see Eq. (2)), both the consumer and the resource populations start to oscillate (see Fig. 2(c)). Thus in presence of dispersal, the coupled system (2) exhibits rhythmic behavior, whereas its uncoupled unit (1) is at a rest state.

Moreover, to explore the generation of oscillation from the excitable steady state we find the relationship between the coupling parameters and the local dynamics (governed by ω) using a two parameter ($\omega - \epsilon$) bifurcation diagram for three different Q values (Fig. 3); the zone below the Hopf bifurcation (HB) curve represents steady state, which yields oscillation through the Hopf bifurcation. From Fig. 3 it is observed that for $\omega > \omega_H$ individual patches are in oscillating zone irrespective of dispersion. But for $\omega < \omega_H$, HB lines become steeper from low to high mean field density (Q). Note that, for low value of mean-field density ($Q = 0.45$), even for low dispersal rate (ϵ), oscillation occurs (see Fig. 3).

Next, we consider two identical patches at their respective steady states and investigate the appearance of oscillations as well as oscillation's transition to coupling induced steady states (both homogeneous and inhomogeneous) through the oscillation quenching mechanisms such as AD and OD in the coupled model (2). Here, identical in the sense that local dynamics of consumer and resource are same for all the patches. In Fig. 4, we depict a one parameter bifurcation diagram with variations in the dispersal rate (ϵ). Here, each fixed ϵ and Q represent a local habitat setup, whereas varying ϵ or Q represents the environmental fluctuations in the local habitat. The qualitative dynamics of the coupled system is identified in this bifurcation diagram for varying dispersal rate. In Fig. 4(a), steady states of the resource (X) are given for varying ϵ with fixed $Q = 0.95$. Other fixed parameters are $\gamma = 0.05$, $\omega = 0.34$, $\nu = 0.053$, and $\beta = 0.43$. It is important to note here that initially we start with a stable steady state instead of oscillatory state in each patch of the uncoupled system. With an increase in the pa-

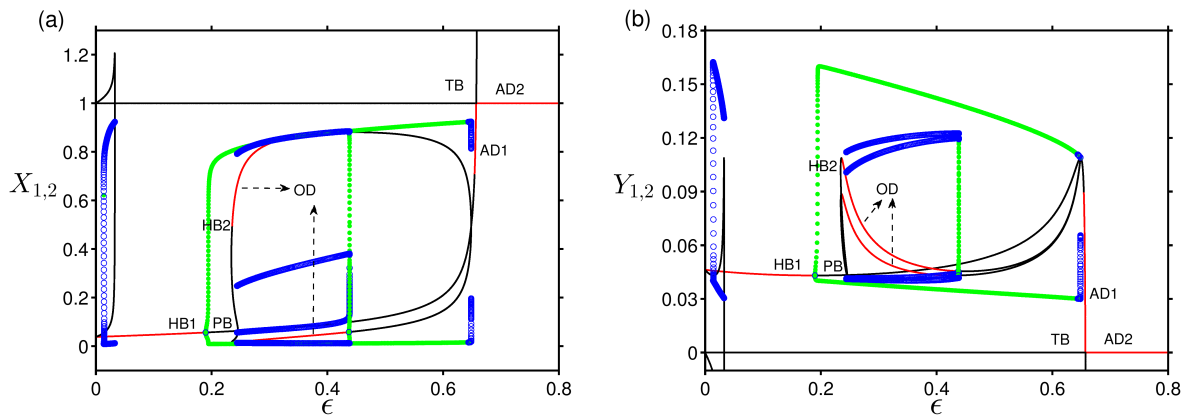


FIG. 4. (Color online) Dispersal induced rhythm and creation of AD and OD; individual patches are in the excitable steady state ($\omega = 0.34$): (a) One parameter bifurcation diagram of the resource (X) for varying coupling strength (ϵ). Here AD, OD, HB, PB and TB represent that amplitude death, oscillation death, Hopf bifurcation, pitchfork bifurcation and transcritical bifurcation, respectively. (b) One parameter bifurcation diagram of the consumer (Y) for varying coupling strength (ϵ). Other fixed parameters are $\gamma = 0.05$, $\nu = 0.053$, $\beta = 0.43$ and $Q = 0.95$. Here green and blue circles represent the stable and the unstable limit cycles, whereas red and black curves represent the stable and the unstable steady states, respectively.

parameter ϵ , a steady state is transformed into oscillatory state at $\epsilon_{HB1} \approx 0.1898$. Further, OD is created by symmetry breaking of the steady state through a pitchfork bifurcation (PB) at $\epsilon_{PB} \approx 0.2456$, whereas AD is created through a transcritical bifurcation (TB) at $\epsilon_{TB} \approx 0.6572$. After the pitchfork bifurcation, OD creates inhomogeneous steady states through the Hopf bifurcation (HB2) at $\epsilon_{HB2} \approx 0.2355$ (shown in Figs. 4(a)). The consumer (Y) dynamics for varying the dispersal rate ϵ are also shown in Fig. 4(b). Notice that, a very small change in ϵ may lead to a critical transition from AD1 to AD2, where suddenly the consumer goes to extinction, i.e., $Y_{1,2} = 0$ (see Fig. 4(b)). Here AD1 represents the non-zero density of both the consumer and the resource whereas AD2 is non-zero density of only the resource and the consumer is extinct from the community. This is due to the fact that at the TB point (i.e., $\epsilon_{TB} \approx 0.6572$ where $X_i = 1$) the resource attains its maximum carrying capacity³⁰. Note that as stable limit cycles share the phase space with the OD state, thus, depending on the initial conditions, we have either stable oscillations or stable steady states. In general, if we vary the dispersal rate ϵ with changing the mean-field density Q , we find similar dynamics, except now the values of bifurcation points change accordingly.

As ω is shifted towards the edge of the oscillation, i.e., ω_H , we find qualitative changes in the bifurcation scenarios. Now, with increasing dispersal rate ϵ , not only we get a transition from steady state to periodic oscillation, but additionally we observe higher periodic oscillations through the period doubling bifurcation of limit cycle. We take $\omega = 0.48$ (remember $\omega_H = 0.528$) and computed one parameter bifurcation diagram (Fig. 5). Importantly, focus the region where the dispersal rate (ϵ) is between 0.04 and 0.06 in Fig. 5 and at this region, the coupled system shows multiple characteristics in a small variation of initial density and dispersal rate.

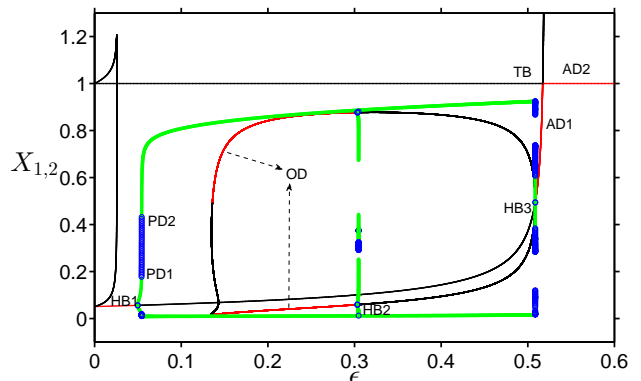


FIG. 5. (Color online) One parameter bifurcation diagram for varying the coupling strength (ϵ) with the fixed mean-field density ($Q = 0.95$). Here PD represents the period-doubling bifurcation. Other parameters are fixed at $\beta = 0.43$, $\nu = 0.053$, $\gamma = 0.05$ and $\omega = 0.48$.

First, period-1 limit cycle is created via a Hopf bifurcation ($HB1$) at $\epsilon_{HB1} \approx 0.04981$. Then the stable period-1 limit cycle becomes unstable and there is a creation of a stable period-2 limit cycle via a period-doubling bifurcation of limit cycle (PD1) at $\epsilon_{PD1} \approx 0.05417$. Further, there is a transition from the stable period-2 limit cycle to a stable period-1 limit cycle via a reverse period-doubling bifurcation of limit cycle (PD2) at $\epsilon_{PD2} \approx 0.05442$. Subsequently, there exists similar oscillatory characteristics in $HB2$ at $\epsilon_{HB2} \approx 0.3032$ with OD.

The phase space and time series for a particular choice of the parameters $\epsilon = 0.054$ (i.e., in between $HB1$ and $PD1$) are shown in Figs. 6(a)-(d). For a small perturbation in initial conditions, we have distinct time period of oscillation of stable period-1 and period-2 limit

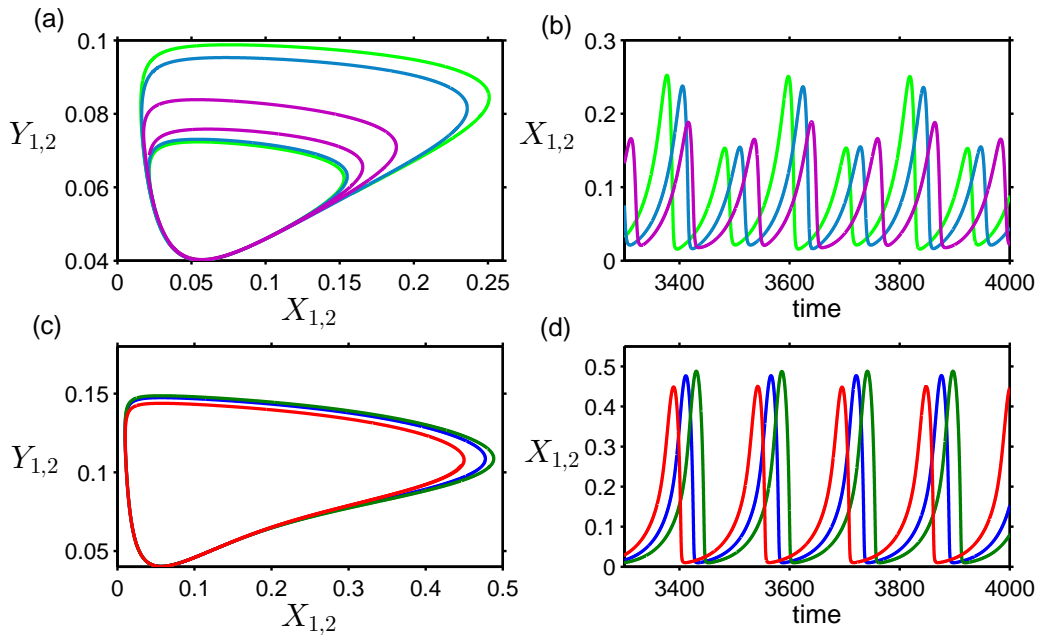


FIG. 6. (Color online) Phase portrait and temporal dynamics exhibiting excitability for fixed $\epsilon = 0.0545$ and $Q = 0.95$: (a) Period-2 limit cycles, where three different initial conditions are chosen around the unstable period-1 limit cycles (i.e., blue circles between PD1 and PD2 in the Fig. 5(a)). (b) Corresponding time series of period-2 limit cycles in (a). (c) Period-1 limit cycle, where three different initial conditions are chosen around the stable limit cycles shown above PD2 in Fig. 5(a). (d) Corresponding time series of period-1 limit cycles in (c). Other parameters are same as in Fig. 5.

cycles. For this parametric set up, the coupled system shows neutral oscillations (i.e. center) since we have different amplitude and time period for each initial condition. Further, there is some threshold in initial condition leads to period-1 limit cycle. Instead of center in the dynamics of oscillation, above a certain threshold in the dispersal rate lead to stable limit cycle. Figs. 6(a) and 6(b) show the phase space and time series of period-2 limit cycles, whereas Figs. 6(c) and 6(d) show the phase space and time series of excitable period-1 limit cycles with different time period of oscillation. In other words, initial conditions for Fig. 6(a) are chosen between the period doubling bifurcations PD1 and PD2 mentioned in the Fig. 5. As the Truscott–Brindley model mimics the plankton algal bloom in aquatic ecosystems, the existence of period-2 cycles resembles the multiyear cycles in aquatic ecosystems³⁴.

From the above results, we have seen that (see Fig. 5) a stable oscillation is always created from an excitable steady state through a supercritical Hopf bifurcation confirming the fact that our present ecosystem belongs to the type-II excitable system.

2. Stability Analysis

Considering the perfect synchrony of the coupled two-patch ecosystem (2), we calculate bifurcation curves/points by using the fixed points of the

coupled system wherever possible. Eqs. (2) has $(0, 0, 0, 0)$ and $(1, 0, 1, 0)$ as trivial fixed points, whereas (X^*, Y^*, X^*, Y^*) is a nontrivial fixed point, where

$$X^* = \sqrt{\frac{\nu^2(\epsilon - Q\epsilon + \gamma\omega)}{\gamma + (Q - 1)\epsilon - \gamma\omega}}, \text{ and}$$

$$Y^* = \frac{-\beta\gamma\nu^2}{(\gamma + (Q - 1)\epsilon - \gamma\omega)} + \frac{\beta\gamma\nu}{\sqrt{(\epsilon - Q\epsilon + \gamma\omega)(\gamma + (Q - 1)\epsilon - \gamma\omega)}}.$$

The Jacobian \mathcal{J}_1 of the system (2) at $(1, 0, 1, 0)$ is given by:

$$\mathcal{J}_1 = \begin{bmatrix} j_{11} & j_{12} & 0 & 0 \\ 0 & j_{22} & 0 & j_{24} \\ \cdots & \cdots & \cdots & \cdots \\ 0 & 0 & j_{11} & j_{12} \\ 0 & j_{24} & 0 & j_{22} \end{bmatrix},$$

where,

$$j_{11} = -\beta, \quad j_{12} = -\frac{1}{1 + \nu^2}, \quad j_{24} = \frac{\epsilon Q}{2}, \quad \text{and}$$

$$j_{22} = -1 + \frac{\epsilon Q}{2} + \gamma \left(\frac{1}{1 + \nu^2} - \omega \right).$$

The eigenvalues of the Jacobian $\mathcal{J}_1|_{(1,0,1,0)}$ are:

$$\lambda_{1,2} = j_{11} = -\beta, \text{ and} \quad (4a)$$

$$\lambda_{3,4} = j_{22} \mp j_{24}. \quad (4b)$$

Solving the eigenvalues $\lambda_{3,4}$ (given by (4b)) for ϵ or γ , we get two bifurcation curves. In particular, solving $j_{22} + j_{24}$ for ϵ gives the transcritical bifurcation (TB) curve of Fig. 5, where:

$$\epsilon_{TB} = \frac{\gamma(\omega - 1 + \nu^2\omega)}{(Q - 1)(1 + \nu^2)}.$$

For the nontrivial fixed point (X^*, Y^*, X^*, Y^*) , the Ja-

cobian matrix \mathcal{J}_2 is given by:

$$\mathcal{J}_2 = \begin{bmatrix} j_{11}^+ & j_{12}^+ & : & 0 & 0 \\ j_{21}^+ & j_{22}^+ & : & 0 & -j_{22}^+ \\ \cdots & \cdots & & \cdots & \cdots \\ 0 & 0 & : & j_{11}^+ & j_{12}^+ \\ 0 & -j_{22}^+ & : & j_{21}^+ & j_{22}^+ \end{bmatrix},$$

where, $j_{12}^+ = \frac{(Q-1)\epsilon}{\gamma} - \omega$, $j_{22}^+ = -\frac{Q\epsilon}{2}$,

$$j_{11}^+ = \frac{2\beta\epsilon(Q-1) \left(\sqrt{\nu^2(\epsilon - Q\epsilon + \gamma\omega)} - \sqrt{\gamma + (Q-1)\epsilon - \gamma\omega} \right)}{\gamma\sqrt{\gamma + (Q-1)\epsilon - \gamma\omega}} + \frac{\beta\gamma \left(-\sqrt{\gamma + (Q-1)\epsilon - \gamma\omega} + 2\omega \left(\sqrt{\gamma + (Q-1)\epsilon - \gamma\omega} - \sqrt{\nu^2(\epsilon - Q\epsilon + \gamma\omega)} \right) \right)}{\gamma\sqrt{\gamma + (Q-1)\epsilon - \gamma\omega}}, \text{ and}$$

$$j_{21}^+ = -2\beta \left(\epsilon - Q\epsilon + \gamma(\omega - 1) + \sqrt{\gamma + (Q-1)\epsilon - \gamma\omega} \sqrt{\nu^2(\epsilon - Q\epsilon + \gamma\omega)} \right).$$

The eigenvalues of the Jacobian $\mathcal{J}_2|_{(X^*, Y^*, X^*, Y^*)}$ are

$$\lambda_{1,2}^+ = \frac{1}{2} \left(j_{11}^+ \mp \sqrt{(j_{11}^+)^2 + j_{12}^+ j_{21}^+} \right), \text{ and} \quad (5a)$$

$$\lambda_{3,4}^+ = \frac{1}{2} \left(j_{11}^+ + 2j_{22}^+ \mp \sqrt{(j_{11}^+ - 2j_{22}^+)^2 + 4j_{12}^+ j_{21}^+} \right). \quad (5b)$$

Solving the real part of the eigenvalues $\lambda_{3,4}^+$ in Eq. (5b) for ϵ with other parameters fixed, we get two Hopf bifurcation (HB1 and HB3) curves of Fig. 5. Due to cumbersome mathematical expressions, we don't mention those bifurcation curves here.

C. Dynamics of the coupled system: Non-identical local dynamics

In real spatial ecosystems, interacting patches are, in general, non-identical³⁵. For example, spatial and environmental heterogeneity due to weather fluctuations make the fragmented habitat heterogeneous³⁶. Here we assume heterogeneous patches by considering distinct conversion efficiency (γ) of the consumer population in each patch and look for the transition from the excitable steady state to oscillation and also to oscillation suppression mechanisms (AD and OD). For mismatch in species local dynamics, we set $\gamma = 0.05$ in patch-1 and $\gamma = 0.057$ in patch-2. Remaining parameters are identical in both the patches.

Slow-fast oscillation occurs here also, but it takes place with combination of both stable and unstable limit cycles. Thus, depending upon the initial condition the system (2) will either converge to a stable limit cycle or to an unstable limit cycle. Figure 7 represents a one parameter bifurcation diagram with variations in ϵ . Here OD

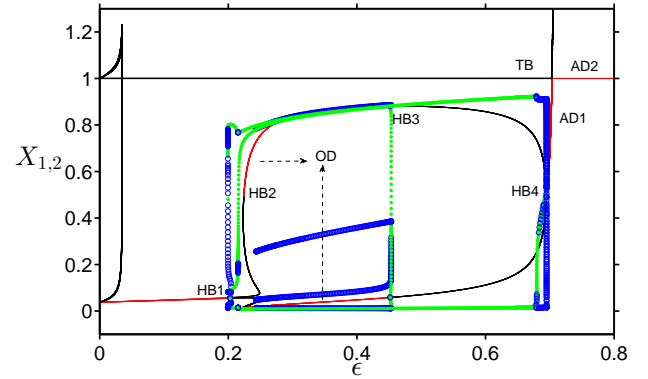


FIG. 7. (Color online) One parameter bifurcation diagram for non-identical patches with variations in ϵ : Resource population densities of $X_{1,2}$ are shown along y -axis. The limit cycles (green and blue circles) in vertical directions represent the excitation which has a different period for distinct initial conditions. Here $\gamma = 0.05$ in patch-1 and $\gamma_2 = 0.057$ in patch-2, and the other parameters are same as in Fig. 4.

is created due to the mismatch in species local dynamics. Apart from the OD and AD states, we have excitable oscillation with vertically distributed green circles and blue circles in the mentioned HB points of Fig. 7. Moreover, wherever Hopf bifurcation occurs (i.e., HB1, HB2, HB3 and HB4), we have slow-fast oscillations in the coupled non-identical patches.

D. Coupling in both resource and consumer

Long term persistence of ecosystem functioning and community structure involve the collective dynamics of

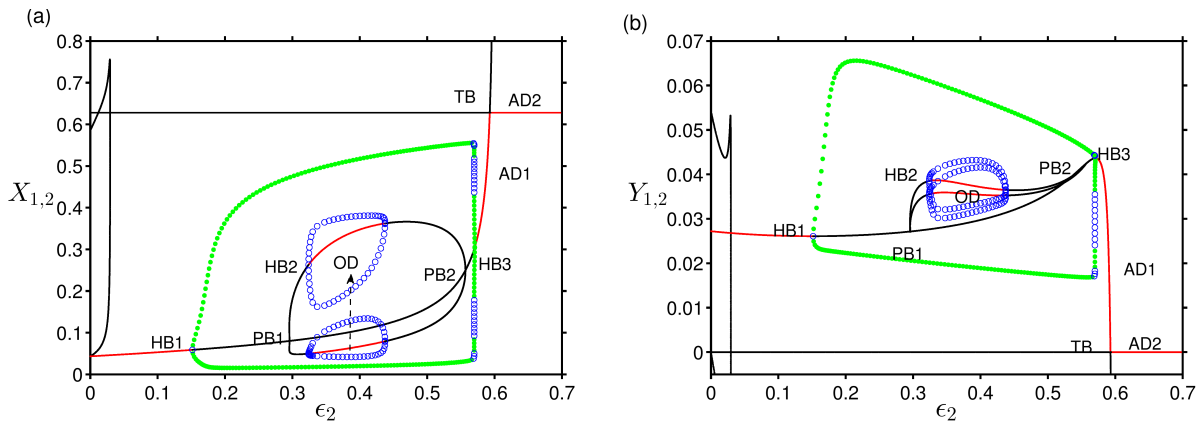


FIG. 8. (Color online) Asymmetric coupling: One parameter bifurcation diagram of: (a) Resource (X_i) for varying the coupling strength ϵ_2 and (b) consumer (Y_i) for varying the coupling strength ϵ_2 . Other fixed parameters are $\beta = 0.43$, $\nu = 0.053$, $\gamma = 0.05$, $\omega = 0.4$, $\epsilon_1 = 0.2$, $Q_1 = 0.2$, and $Q_2 = 0.95$.

species distribution and subsequently, to shape the biodiversity, organisms movement plays important role³⁷. As every organism depends on the other for their resource in most of the terrestrial and aquatic ecosystems, while dispersal of the consumer takes place for favorable conditions, passive dispersal happens in the resource also (i.e., instead of moving, it's being moved either directly or indirectly). Moreover, the complexity of food web dynamics and it's associated interactions involve the dispersal of all the species presence in the ecosystem^{13,38}. So the collective excitable dynamics can be strengthened if we consider the coupling in both the variables X_i and Y_i . Instead of only the consumer movement to check the excitability in the Truscott–Brindley model (1), we consider the more natural dispersal (i.e., when both species are coupled with mean-field assumption) by setting distinct dispersal rate and mean-field density in consumer–resource populations. The coupled TB model now becomes:

$$\frac{dX_i}{dt} = \beta X_i(1 - X_i) - Y_i \frac{X_i^2}{X_i^2 + \nu^2} + \epsilon_1 (Q_1 \bar{X} - X_i), \quad (6a)$$

$$\frac{dY_i}{dt} = \gamma \left(\frac{X_i^2}{X_i^2 + \nu^2} - \omega \right) Y_i + \epsilon_2 (Q_2 \bar{Y} - Y_i), \quad (6b)$$

where $i = 1, 2, \dots, N$, $\bar{X} = \frac{1}{N} \sum_{i=1}^N X_i$ and $\bar{Y} = \frac{1}{N} \sum_{i=1}^N Y_i$.

Here ϵ_1 and ϵ_2 represent the dispersal rate of the resource X_i and the consumer Y_i , respectively, whereas mean-field density of X_i and Y_i are Q_1 and Q_2 , respectively.

1. Asymmetric coupling between two patches

Recently, trait-based approaches have been used to predict various consequences of ecological communities^{39,40}. In ecosystems, characteristics of

each community differs as per environmental conditions due to spatiotemporal heterogeneity in the habitat by their nature. So it is natural that the dispersal rate at the consumer level can differ from the dispersal rate at the resource level. As symmetric coupling is a special case of the more general situation of asymmetric coupling, hence, in spatial parameters, we use asymmetric coupling in the dispersal rate and the mean-field density, i.e., $\epsilon_1 \neq \epsilon_2$ and $Q_1 \neq Q_2$ ³². We check the coupled system dynamics for varying dispersal rate of consumer (ϵ_2) where other spatial parameters are fixed at $\epsilon_1 = 0.2$, $Q_1 = 0.2$ and $Q_2 = 0.95$ with the identical local dynamics in each patch.

Here AD and OD occurs along with slow-fast oscillations. Figs. 8(a) and 8(b) show both appearance and disappearance of oscillations using one-parameter bifurcation diagram of the resource (X) and the consumer (Y) for varying dispersal rate of the consumer (ϵ_2). Although we start with steady state in the uncoupled model, in the coupled system, creation of oscillations occurs at HB1 ($\epsilon_{HB1} \approx 0.1516$). Further, here also OD is created by symmetry breaking of steady state through pitchfork bifurcation (PB1) at $\epsilon_{PB1} \approx 0.2957$. Further, after HB3 (at $\epsilon_{HB3} \approx 0.5706$), oscillations are suppressed and give raise to homogeneous steady state (AD1). Interestingly, a small increase in dispersal rate leads to the transition from AD1 to AD2 through transcritical bifurcation (TB) at $\epsilon_{TB} \approx 0.5929$.

Figure 9 shows two-parameter bifurcation diagrams those identify the occurrence oscillations for each dispersal rate through HB. For asymmetric coupling, this is shown in Figs. 9(a) and 9(b) with $\omega - \epsilon_1$ and $\omega - \epsilon_2$ planes respectively. In fact, here steady states only occur in the red shaded region and oscillation starts at HB point whereas light color shaded region is for coexistence of oscillation along with AD and OD states. Moreover, even though we have started with fixed point in the uncoupled system, in Fig. 9(a), oscillation arises in light color

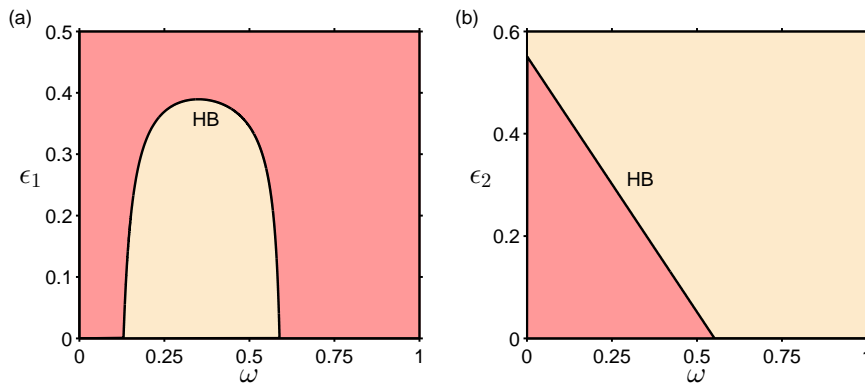


FIG. 9. (Color online) Generation of Oscillation : (a) Oscillations due to asymmetric coupling for the fixed parameters $\epsilon_2 = 0.4$, $Q_1 = 0.2$ and $Q_2 = 0.95$, (b) oscillations are created at HB due to asymmetric coupling with fixed parameters $\epsilon_1 = 0.2$, $Q_1 = 0.2$ and $Q_2 = 0.95$. Here, the red shaded region represents the occurrence of only fixed steady states, HB curve represents the point where the oscillation starts due to the coupling and light color shaded region after HB curve is the region of both appearance and disappearance of oscillations. Other fixed parameters are $\beta = 0.43$, $\nu = 0.053$, $\omega = 0.34$ and $\gamma = 0.05$.

shaded region even at $\epsilon_1 = 0$ due to the dispersal of species from the other patch (i.e., $\epsilon_2 \neq 0$).

2. A network with more than two patches

As spatial movement of species takes place in a large number of patches in natural ecosystems, we consider a network (6) with $N = 32$ patches where dispersal takes place in both the populations. Moreover, both spatial and environmental heterogeneity are taken into account and we analyze the mean-field coupled network in two distinct cases.

Case-I: First, we consider asymmetry in the spatial parameters (i.e., ϵ_i and Q_i) with identical local dynamics, i.e., in Eqs. (6) we consider $\epsilon_1 \neq \epsilon_2$ and $Q_1 \neq Q_2$. In this case, the creation of oscillation, AD and OD are still possible. The spatiotemporal dynamics of oscillation generation is shown in Figs. 10(b) and 10(g), whereas the dynamics of its uncoupled version is shown in Figs. 10(a) and 10(f). When there is no dispersal, each patch is in a steady state, then dispersal makes the network of connected patches to show the synchronized oscillation which is further suppressed to AD/OD. Here, the spatiotemporal dynamics of AD is shown in Figs. 10(c) and 10(h) for $\epsilon_1 = 0.2$, $\epsilon_2 = 0.5875$, $Q_1 = 0.2$ and $Q_2 = 0.95$, whereas spatiotemporal dynamics of OD is shown in Figs. 10(d) and 10(i) for the parameters $\epsilon_1 = 0.2$, $\epsilon_2 = 0.5145$, $Q_1 = 0.2$ and $Q_2 = 0.95$.

Case-II: Next, we use mismatch in species local dynamics together with asymmetric coupling. In particular, we set mismatch in consumer's conversion efficiency (γ) for all $N = 32$ patches. We choose the mismatch in each patch in the following way: $\gamma_i = (1 + \frac{i}{100})\gamma_0$, where $i = 1, 2, \dots, 32$ and $\gamma_0 = 0.05$. Due to mismatch in species local dynamics, inhomogeneous steady states are created and thus forms a multi-clustered OD state which is shown in Figs. 10(e) and 10(j) for the param-

eters $\epsilon_1 = 0.2$, $\epsilon_2 = 0.608$, $Q_1 = 0.2$ and $Q_2 = 0.95$. In multi-clustered OD state, populations populate in different steady states and the position of those steady states may change depending upon the choice of γ_i and the initial conditions.

Thus, Fig. 10 generalizes the results of this excitable system by depicting the spatiotemporal dynamics starting from steady states of the uncoupled system, creation of oscillations and its transition to oscillation suppression such as AD and OD with 2-cluster and multi-clustered states when both populations are coupled. However, if dispersal takes place in only one species, the qualitative dynamics remains same. Also the qualitative nature of the network remains same if one considers more number of patches.

IV. DISCUSSION AND CONCLUSION

In summary, in this paper we have explored the emergent behaviors of an excitable ecological network local dynamics where the dynamics in each node are governed by the Truscott–Brindley model. The connections between the nodes are governed by the mean-field dispersion. We have emphasized on the interplay of excitability and dispersal by always considering that the individual patches are in their (excitable) steady states. Unlike previous studies,^{41,42} we have not only observed the generation of oscillation (or so called rhythmogenesis) but we have also reported two distinct mechanisms of cessation of oscillations, namely amplitude and oscillation death. We have analyzed various dynamical aspects of dispersion using spatial and environmental heterogeneity. At first, considering dispersal only in the consumer population and also the local habitat's interconnection, the generation of oscillations is identified in the coupled system from their respective steady states. The mean-field dispersion assumption used here, resembling as a globally coupled

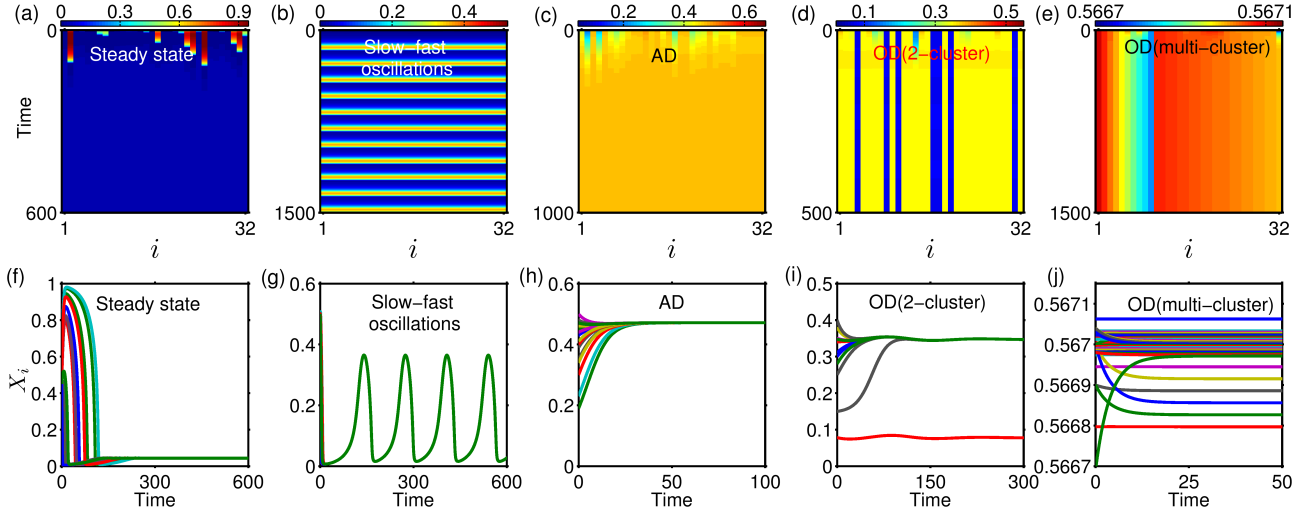


FIG. 10. (Color online) Dynamics of a network with $N = 32$ nodes (i.e., patches): (a) Steady states of 32-patches when uncoupled for the fixed parameters $\epsilon_1 = \epsilon_2 = 0$, (b) Slow-fast oscillations through asymmetric coupling for the fixed parameters $\epsilon_1 = 0.2$ and $\epsilon_2 = 0.1647$, (c) AD due to asymmetric coupling for the fixed parameters $\epsilon_1 = 0.2$ and $\epsilon_2 = 0.5875$, (d) OD for asymmetric coupling with identical local dynamics in 32 patches for the parameters $\epsilon_1 = 0.2$ and $\epsilon_2 = 0.5145$, (e) OD with multi-cluster due to mismatch in local dynamics with parameters $\epsilon_1 = 0.2$ and $\epsilon_2 = 0.608$. In (f)-(j) are the time series corresponding to the spatial dynamics shown in (a)-(e) respectively. Other fixed parameters are $Q_1 = 0.2$ and $Q_2 = 0.95$, $\beta = 0.43$, $\nu = 0.053$, $\gamma = 0.05$ and $\omega = 0.4$.

excitable system, potentially determines the qualitative behaviors of slow-fast dynamical systems along with excitation. Typically, the dispersal between the patches influences the intrinsic dynamics of the system resulting multiple oscillatory dynamics such as period-1, period-2 limit cycles, center and stable limit cycle. Moreover, the excitable dynamics due to variation of only initial conditions in the interacting habitats show synchronized stable oscillations with distinct time period of oscillations. It is important to note that the population movement changes the intrinsic dynamics of the uncoupled system and promotes generation of oscillation in the coupled system. While the species dispersion between the patches generate the oscillations by exhibiting the type-II excitability in the coupled Truscott–Brindley model, on contrary, the same coupling feature is used to suppress the oscillations. In fact, the multiple oscillation suppression states, namely AD and OD highlight the transition of oscillation to stable homogeneous and inhomogeneous steady states respectively in a homogeneous patchy habitat. Essentially, the mean-field coupling constitutes both appearance and disappearance of oscillations alongside excitable dynamics both in identical and non-identical patches.

On the other hand, the consumer and the resource dispersal are taken into account, we have analyzed the consequences of excitability through asymmetric coupling along with a network of globally connected patches. Our findings indicate that the combined effect of species dispersion for varying species local dynamical parameters as well as spatial parameters also determines the excitability. In addition to that, oscillation quenching

states (AD and OD) are determined in both homogeneous and heterogeneous habitats. Overall, in all the results, we have started with steady states in an uncoupled Truscott–Brindley model and then moved to oscillatory state through mean-field coupling and further transitioned to stable steady states (i.e., AD and OD). This dynamical phenomena of back and forth behavior of steady state to oscillations is valid for a large number of connected nodes (i.e., patch) also. So the species dispersal can self-assemble the ecological communities among the fragmented habitats which prevents the complete extinction of local species. However, instead of starting from steady state in the uncoupled Truscott–Brindley model, if each individual patch is in oscillatory state, then the oscillation quenching mechanisms of the coupled system is still valid. In fact, the excitation with AD and OD is also valid in that case.

While the long term dynamics of plankton organisms is based on the dynamics of Truscott–Brindley model, the dispersion phenomena has significant effect in structuring the community in ecosystems. However, the environmental fluctuations as a stochastic effect have an impact in climatic dynamics due to the seasonal cycles variation of planktonic organisms. In line with the reason that the tininess of plankton organisms, mean-field description is a suitable one to study the species density in plankton ecosystems^{3,43}. Considering the dispersal as like fluctuations, our coupled Truscott–Brindley model localizes the populations regionally through mean-field description and show the excitability with various behaviors of limit cycles due to perturbation. Hence our findings may be

helpful for the regulation and the restoration of the stable as well as the oscillatory populations using the back and forth behavior of coupling features. Overall, the mean-field description enables both rhythmic and steady state behaviors of an ecological system. Further the complexity of the system increases for different network of connected habitats and thus detailed study is involved with various coupling aspects to hold this mechanisms of appearance and disappearance of oscillations.

ACKNOWLEDGMENTS

T.B. acknowledges the financial support from SERB, Department of Science and Technology (DST), Govt. of India [grant: SB/FTP/PS-005/2013]. P.S.D. acknowledges financial support from SERB, Department of Science and Technology (DST), Govt. of India [grant: YSS/2014/000057].

- ¹A. Longtin, *Chaos, Solitons & Fractals* **11**, 1835 (2000).
- ²A. Franci, G. Drion, V. Seutin, and R. Sepulchre, *PLoS Computational Biology* **9**, e1003040+ (2013).
- ³P. Olla, *Physical Review E* **87**, 012712 (2013).
- ⁴B. Lindner, J. García-Ojalvo, A. Neimand, and L. Schimansky-Geiere, *Physics Reports* **392**, 321 (2004).
- ⁵A. Keane, T. Dahms, J. Lehnert, S. A. Suryanarayana, P. Hövel, and E. Schöll, *The European Physical Journal B* **85** (2012).
- ⁶C. R. Laing, B. Doiron, A. Longtin, L. Noonan, R. W. Turner, and L. Maler, *Journal of Computational Neuroscience* **14**, 329 (2003).
- ⁷E. M. Izhikevich, *International Journal of Bifurcation and Chaos* **10**, 1171 (2000).
- ⁸J. E. Truscott and J. Brindley, *Bulletin of Mathematical Biology* **56**, 981 (1994).
- ⁹J. H. Steele, *Nature* **313**, 355 (1985).
- ¹⁰P. Chesson and N. Huntly, *The American Naturalist* **150**, 519 (1997).
- ¹¹O. N. Bjørnstad and B. T. Grenfell, *Science* **293**, 638 (2001).
- ¹²G. Walther, E. Post, P. Convey, A. Menzel, C. Parmesan, T. J. C. Beebee, J. Fromentin, O. Hoegh-Guldberg, and F. Bairlein, *Nature* **416**, 389 (2002).
- ¹³P. Amarasekare, *Annual Review of Ecology, Evolution, and Systematics* **39**, 479 (2008).
- ¹⁴B. Blasius, A. Huppert, and L. Stone, *Nature* **399**, 354 (1999).
- ¹⁵D. Tilman and P. Kareiva, *Spatial Ecology: The Role of Space in Population Dynamics and Interspecific Interactions* (Princeton University Press, Princeton, New Jersey, 1998).
- ¹⁶K. Shea and P. Chesson, *Trends in Ecology & Evolution* **17**, 170 (2002).
- ¹⁷T. Banerjee, P. S. Dutta, and A. Gupta, *Physical Review E* **91**, 052919 (2015).
- ¹⁸A. Morozov and S. Petrovskii, *Bulletin of Mathematical Biology* **71** (2009).
- ¹⁹T. Banerjee and D. Biswas, *Chaos* **23**, 043101 (2013).
- ²⁰T. Banerjee and D. Ghosh, *Phy. Rev. E* **89**, 052912 (2014).
- ²¹T. Banerjee and D. Ghosh, *Phy. Rev. E* **89**, 062902 (2014).
- ²²S. H. Strogatz, *Nature* **410**, 268 (2001).
- ²³A. Koseska, E. Volkov, and J. Kurths, *Physics Reports* **531**, 173 (2013).
- ²⁴A. Koseska, E. Volkov, and J. Kurths, *Physical Review Letters* **111**, 024103 (2013).
- ²⁵A. Koseska, E. Volkov, and J. Kurths, *Euro. Phys. Lett.* **85**, 28002 (2009).
- ²⁶A. Koseska, E. Volkov, and J. Kurths, *Chaos* **20**, 023132 (2010).
- ²⁷A. Koseska, E. Ullner, E. Volkov, J. Kurths, and J. García-Ojalvo, *J. Theoret. Biol.* **263**, 189 (2010).
- ²⁸R. Karnatak, R. Ramaswamy, and U. Feudel, *Chaos, Solitons & Fractals* **68**, 48 (2014).
- ²⁹A. M. Edwards, *Journal of Plankton Research* **23**, 389 (2001).
- ³⁰W. W. Murdoch, C. J. Briggs, and R. M. Nisbet, *Consumer-Resource Dynamics* (Princeton University Press, Princeton, New Jersey, 2003).
- ³¹I. Hanski, *Metapopulation Ecology* (Oxford University Press, USA, 1999).
- ³²R. Arumugam, P. S. Dutta, and T. Banerjee, *Chaos* **25**, 103121 (2015).
- ³³B. Ermentrout, *Simulating, Analyzing, and Animating Dynamical Systems: A Guide to Xppaut for Researchers and Students (Software, Environments, Tools)* (SIAM Press, 2002).
- ³⁴C. A. Klausmeier and E. Litchman, *The American Naturalist* **180**, 1 (2012).
- ³⁵M. Holyoak, M. A. Leibold, and R. D. Holt, *Metacommunities: Spatial Dynamics and Ecological Communities* (University of Chicago Press, Chicago, 2005).
- ³⁶P. Opdam and D. Wascher, *Biological Conservation* **117**, 285 (2004).
- ³⁷F. Jeltsch, D. Bonte, G. Pe'er, B. Reineking, P. Leimgruber, N. Balkenhol, B. Schröder, C. Buchmann, T. Mueller, N. Blaum, D. Zurell, K. Bohning-Gaese, T. Wiegand, J. Eccard, H. Hofer, J. Reeg, U. Eggers, and S. Bauer, *Movement Ecology* **1** (2013).
- ³⁸K. S. McCann, J. B. Rasmussen, and J. Umbanhowar, *Ecology Letters* **8**, 513 (2005).
- ³⁹E. Acevedo-Trejos, G. Brandt, J. Bruggeman, and A. Merico, *Scientific Reports* **5**, 1 (2015).
- ⁴⁰A. Merico, G. Brandt, S. L. Smith, and M. Oliver, *Frontiers in Ecology and Evolution* **2**, 1 (2014).
- ⁴¹T. Singla, N. Pawar, and P. Parmananda, *Physical Review E* **83** (2011).
- ⁴²M. Dasgupta, M. Rivera, and P. Parmananda, *Chaos* **20**, 023126 (2010).
- ⁴³A. Morozov and J. C. Poggiale, *Ecological Complexity*, 2012 **10**, 1 (2012).